ACCEPTED MANUSCRIPT

Structural and electrical properties of ferroelectric poly(vinylidene fluoride) and mechanically activated ZnO nanoparticle composite films

Structural and electrical properties of ferroelectric poly(vinylidene fluoride) and mechanically activated ZnO nanoparticle composite films

A.Peleš[1], O. Aleksić[2], V. P. Pavlović[3], V. Djoković[4], R. Dojčilović[4], Z. Nikolić[5], F. Marinković[5], M. Mitrić[4], V. Blagojević[1], B. Vlahović[6,7], V. B. Pavlović[1]

[1]*Institute of Technical Sciences of SASA, Knez Mihailova 35/IV 11000 Belgrade, Serbia*

[2]*Institute for Multidisciplinary Research, University of Belgrade, 11000 Belgrade, Serbia*

[3]*Faculty of Mechanical Engineering, University of Belgrade, 11000 Belgrade, Serbia*

[4]*Vinča Institute of Nuclear Sciences, University of Belgrade, P.O. box 522, 11001 Belgrade, Serbia*

[5]*Faculty of Physics, University of Belgrade, Studentski trg 12-16, 11000 Belgrade, Serbia*

[6]*North Carolina Central University, Durham, NC 27707, USA*

[7]*NASA University Research Center for Aerospace Device Research and Education and NSF Center of Research Excellence in Science and Technology Computational Center for Fundamental and Applied Science and Education, NC, USA*

Abstract

The influence of the mechanical activation of ZnO nanoparticle fillers on the structural and electrical properties of the matrix of poly(vinylidenefluoride)-ZnO (PVDF-ZnO) films was investigated. Transmission electron microscopy and scanning electron microscopy analyses showed that mechanical activation in a high energy planetary ball mill reduces the size of ZnO particles. X-ray diffraction and Raman spectroscopy revealed that PVDF crystallized predominantly as the γ-phase. Non-activated ZnO filler reduces the degree of the crystallinity of the matrix and promotes crystallization of α-phase of PVDF in the film, while the fillers activated for 5 and 10 min induce crystallization of β-phase, indicating that mechanical activation of the filler can be used as a general method for fabrication of PVDF composites with increased content of piezoelectric β-phase crystals. Dielectric spectroscopy measurements show that polymer composite with the high content of β-phase (with ZnO filler activated for 5 min) exhibits the highest value of dielectric permittivity in 150-400 K range of temperatures. Kinetic analysis shows combined effects of increased surface area and increased concentration of surface defects on the interactions between polymer chains and activated nanoparticles.

Keywords: polymer composites; mechanical activation; crystallization; dielectric properties; PVDF; ZnO

1

Introduction

Poly(vinylidene fluoride) (PVDF) is a semi-crystalline polymer with excellent pyro-and piezo-electric properties [1,2]. Compared to piezoelectric ceramics, PVDF has lower dielectric permittivity but offers certain advantages for sensing applications due to low density, flexibility and toughness. Also, being an engineering plastic, it can easily be processed into technologically useful forms [3,4]. For this reason, polyvinylidene fluoride (PVDF) has been widely used in MEMS technology as well as for ultrasound transducer and medical ultrasound applications. PVDF may crystallize in five distinct crystalline phases, usually denoted as α, β, γ, δ and ε [5,6]. The most common α-phase, typically formed during the crystallization from melt, is characterized by alternating s-trans and s-gauche bonds (TGTG), hence it is non-polar. Both β and γ phases are electroactive, but β-phase exhibits the strongest ferroelectric response due to a particular crystal structure, with all C-C bonds in the trans conformation (TTTT) [6,7]. Therefore, considerable research effort has been devoted to optimization of the conditions that will induce β-phase crystallization in PVDF films [8-13].

One of the methods suggested was mixing of PVDF with nanostructured fillers (montmorillonite, SiO_2 etc.), which would act as nucleation centres for crystallization of the β-phase [12,13]. Addition of carbon nanofibers was found to have a considerable impact on phase composition and crystallization of the β-phase [14]. It was also found that the combination of two fillers (multi-walled carbon nanotubes and polypyrrole) may exhibit a synergistic effect on the hybrid system's electrical properties, due to specific changes in morphology [15-17]. In addition, the application of a stretching process resulted in crystallization of almost pure β-phase (>96%) in both PVDF and PVDF-carbon nanofiber composites [18]. Given that the combination of dielectric fillers and PVDF matrix has been shown to be a good route towards increasing the dielectric permittivity of the material, the introduction of high-dielectric permittivity fillers such as barium titanate, $BaTiO_3$, represented a next logical step [19-23]. However, it was shown that high $BaTiO_3$ contents (20-40%) are necessary to achieve a significant increase in dielectric permittivity [24], while the particles tend to agglomerate in the low surface energy polymer matrix, which can reduce the dielectric strength by triggering percolation effects. In order to improve the dispersion of the $BaTiO_3$ particles in the PVDF matrix, and consequently improve the dielectric strength, their surface can be modified with pentafluorobenzylphosphonic acid [20] or fluoroalkylsilane [25]. The observed increase in the values of dielectric permittivity of the composites was mainly due to the contribution of the filler, however, these studies do not report on the effect of ceramic nanoparticles on the crystallization of different phases in the PVDF.

ZnO is semiconductor with wide direct band gap (3.37eV) and large excitation binding energy at room temperature and finds applications as a material for gas sensors, solar cells, display screens, photocell electrodes and UV-light emitting diodes [26-30]. Nanostructured ZnO [31] has been considered as a good filler material for the fabrication of polymer nanocomposites, due to high dielectric permittivity and good physical properties. Recent studies report that the mixing of ZnO nanoparticles with PVDF may result in interesting optical and electrical properties of the obtained nanocomposite films [32, 33]. However, in spite of improved properties of the films after the introduction of the filler, ZnO nanoparticles have not induced changes in phase crystallization (i.e. post-crystallization phase composition) of PVDF matrix. Another approach suggested was to use PVDF co-polymers such as poly(vinylidene fluoride-trifluoroethylene) (PVDF-TrFE) as a matrix for ZnO nanoparticles [34, 35]. The presence of the trifluoroethylene co-monomers in the macromolecular chains favours β-phase

2

crystallization of PVDF monomers and the ZnO will additionally improve the piezoelectric properties of the films [36].

In our previous studies [37, 38], it was shown that mechanical activation of $BaTiO_3$ filler particles prior to mixing with PVDF may favour β-phase crystallization in the matrix. Mechanical activation was used to reduce the size of $BaTiO_3$ particles, without affecting their ferroelectric tetragonal crystal structure [39]. In this way, the filler could increase the dielectric permittivity due to its higher dielectric permittivity, and through pronounced crystallization of polar β-phase crystals, achieving the same effect on the dielectric permittivity using lower concentrations of the filler. Unlike in the case of nanostructured organosilicate fillers [12, 13], reduction of the size of the ceramic particles prior to their mixing with PVDF does not necessarily lead to a significant increase in dielectric permittivity of the composite, suggesting that the small size of ceramic particles of the filler is not the sole necessary condition for the β-phase crystallization of the PVDF [23]. In addition to the small diameter of $BaTiO_3$ particles, their active surfaces play a crucial role in the nucleation processes that result in formation of β-phase crystals [37, 38]. Here we conducted a study with another type of particles, zinc oxide (ZnO), to investigate whether mechanical activation can be used as a general method for the surface modification of the filler that may induce crystallization of β-phase upon its mixing with PVDF. In addition, the effect of mechanical activation of the filler on dielectric properties of the composites will be investigated.

Experimental

Poly(vinylidene fluoride) (M_w ~ 530 000) and ZnO powder (99.9% p.a.) were purchased from Sigma Aldrich and used without further purification. ZnO powder was mechanically activated for 5 and 10 minutes in a Fritch Pulverissete 5 high energy planetary ball mill with wolfram carbide ball. Ball to sample mass ratio was 40:1, rotation speed 390 rpm. PVDF solution (2wt.%) was prepared by dissolving 3 g of polymer in 150 ml dimethyleformamide (DMF). Non-activated and mechanically activated ZnO powders (0.1 g) were dispersed in 50 ml DMF and sonicated in a BransonW-450 D Digital Sonifier for 20 min at 20% amplitude (80 W). After that, 18.75 ml of ZnO dispersions were mixed with 30 ml of the 2wt.% PVDF solutions. PVDF and nanocomposite films (50 μm) were obtained by casting the solutions into Petri dishes.

Morphology of ZnO powders and PVDF-ZnO nanocomposite films was investigated by a transmission electron microscope (JEOL 100CX II instrument) at 100 kV and electron scanning electron microscope (JEOL JSM-6390) at 10 kV. For TEM measurements ZnO powders were dispersed in alcohol and deposited on the carbon coated copper grid mash. For SEM analyses, PVDF-ZnO nanocomposite films were fractured after immersion in liquid nitrogen and covered with gold. X-ray diffraction patterns of the composites were obtained on a Philips PW-1050 diffractometer with $Cu-K_\alpha$ radiation and a step/time scan mode of 0.05 °/s, in Bragg-Brentano geometry. Notation of the samples and preparation conditions are given in Table I in the text.

Raman scattering measurements were performed on a fully automated Raman microscope (Horiba JobinYvon Lab Ram ARAMIS) using He–Ne laser at 633 nm. The samples were measured under a microscope using a 100× objective. The data were collected over the Raman shift range of 200–3200 cm^{-1}, using a count time of 5 s with 5 averaging cycles and 1800 lines/mm grating.

Dielectric spectroscopy measurements were performed in a shielded cell, with circular electrodes (D = 13 mm). Samples in the form of discs (thickness d = 0.03mm) were cut from the middle of the sheets. Conductance (G) and susceptance (B) were measured as the real part, G, and the imaginary part, B, of AC

conductivity, using the C_p mode of the instrument ($Y = G + iB$). The measurements were performed on a Hameg 8118 instrument in the frequency range from 60 Hz to 60 kHz and in the temperature range from 150 to 400 K using Temperature Controller Lake Shore 340. The heating rate and the acquisition step were 2 K min^{-1} and 10 K, respectively, while the applied voltage was 1.5 V. The characteristic dielectric parameters were calculated using the following relations: tan $\delta = G/B$ and $B = 2\pi fC$, where f is frequency and C is the capacity. In addition, $C = \varepsilon'\varepsilon_0 S/d$, where S/d describes the geometry of the samples ($S = \pi D^2/4$), ε' is the real part of dielectric permittivity and ε_0 is the vacuum permittivity.

Fourier transform infrared (FTIR) spectroscopy was conducted using KBr pellets in 500-4000 cm^{-1} region with Nicolet 6700 FTIR spectrometer (Thermo Scientific, USA).
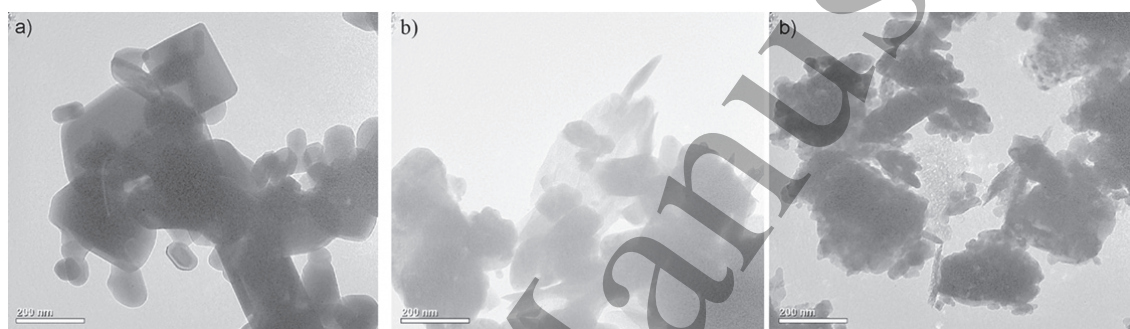
Results and discussion

Figure 1. TEM micrographs of a) non-activated ZnO powder, b) ZnO powder mechanically activated for 10 minutes (both images).

Mechanical activation of ZnO powder is expected to cause a decrease in particle size [40] and an increase in mesopore volume and non-monotonic trends of specific surface area with prolonged milling, caused by powder particle adhesion and breakage due to mechanical activation [41]. TEM micrographs of non-activated and mechanically activated (30 min) ZnO powders are shown in Figure 1. Non-activated ZnO powder consists mostly of particles of regular rectangular or hexagonal shape, which is consistent with hexagonal ZnO phase (Figure 1a). Mechanically activated sample shows irregularly shaped particles where smaller particles exhibit, most likely due to highly activated surfaces, a tendency to agglomerate around larger particles (Figure 1b).

Table I. Notation of the samples, preparation conditions and the average crystal sizes and microstrain of the filler powders. Complete Rietveld refinement is shown in Figure 3.

Sample	wt.% ZnO powder	Mechanical activation time	Average crystallite size of ZnO (nm)	Microstrain (%)
PVDF	0	/	/	/
P5Z0	5	0	61±4	0.53±0.02
P5Z5	5	5	49±3	0.74±0.02
P5Z10	5	10	44±3	0.93±0.02

Rietveld analysis of XRD spectra (presented below) showed a decrease in ZnO crystallite size from ~ 61 to 44 nm and an increase in microstrain up to 0.93%, due to creation of defects during prolonged mechanical activation (Table I).
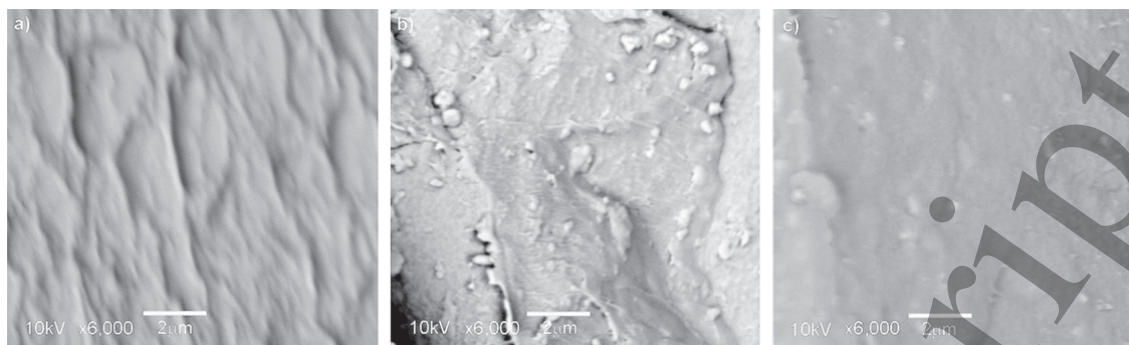
4

Figure 2. SEM micrographs of the fractured surfaces of a) PVDF, b) P5Z0 and c) P5Z10

Figure 2 shows SEM micrographs of fracture surfaces of PVDF and PVDF-ZnO composites with non-activated and mechanically activated (10 min) ZnO fillers. The fracture surfaces of the composites show presence of ZnO agglomerates on the surface of the polymer and inside the polymer matrix, which appear as micrometer-sized particles in SEM images. Sample with non-activated filler exhibits more surface agglomerates (Figure 2b), while sample with activated filler appears to exhibit smoother surface (resulting in lower contrast), suggesting much better dispersion of ZnO particles inside the polymer matrix for filler activated for 10 min (Figure 2c).
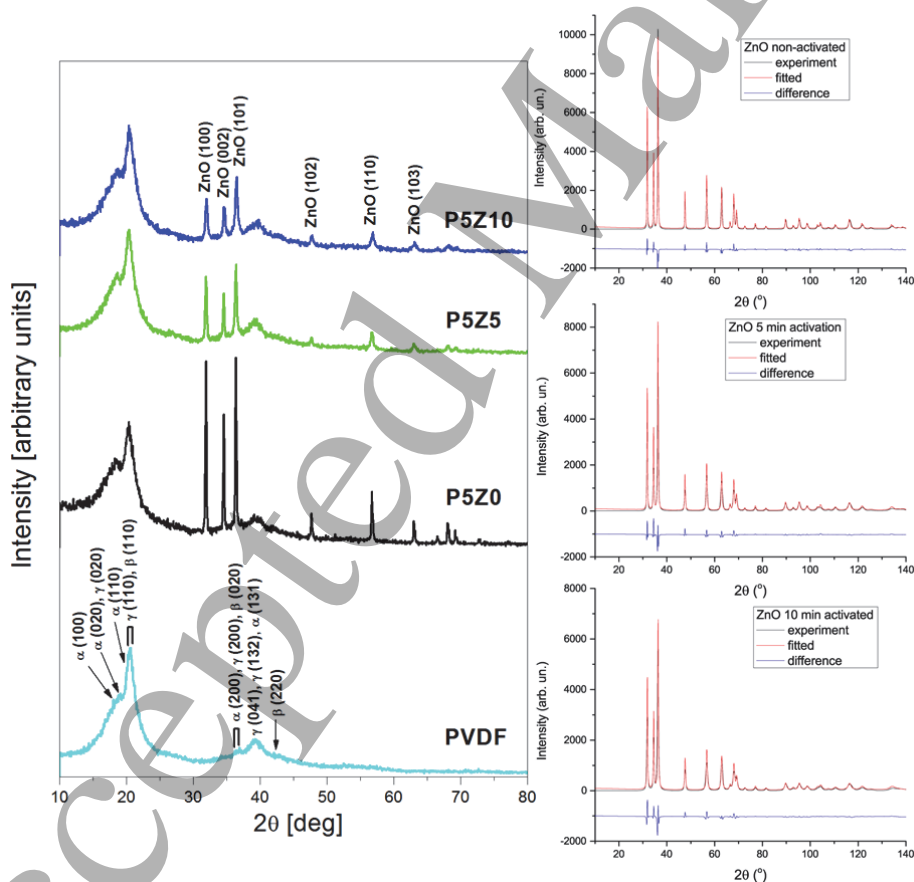

Figure 3. XRD patterns of PVDF and PVDF-ZnO composites with 5 wt% of non-activated and mechanically activated fillers. Rietveld analysis of non-activated and activated ZnO filler powders is shown right (results are shown in Table I).

XRD patterns of the PVDF and PVDF-ZnO composites with 5 wt.% of non-activated and mechanically activated (5 and 10 min) filler are shown in Figure 3. In the diffraction pattern of PVDF, all three phases, α, β and γ [corresponding JCPDS (Joint Committee on Powder Diffraction Standards) database card numbers are JCPDS 42-1650, 38-1638 and 42-1649], are present, with the pronounced contribution of γ-phase. There is also a broad peak from the amorphous phase at low 2θ, suggesting relatively significant volume of the amorphous phase in the samples. In addition, the peaks of PVDF phases appear to be relatively broad, making phase composition analysis difficult. XRD patterns of PVDF-ZnO composites show additional peaks of hexagonal ZnO phase. ZnO diffraction lines, assigned to (100), (002), (101) reflections, become broader as the activation time increases due to reduced size of the ZnO particles and more pronounced lattice distortions [39]. Taking into account very small differences between the positions of γ (110) and β (110) reflections (~ 20.2° versus ~ 20.6°), and no visible peak at β (220) position, XRD analysis could not provide information on the changes in phase composition of PVDF, induced by non-activated and mechanically activated fillers. For this reason, Raman spectroscopy, which is much more sensitive to changes in the crystal structures within polymer, was performed.
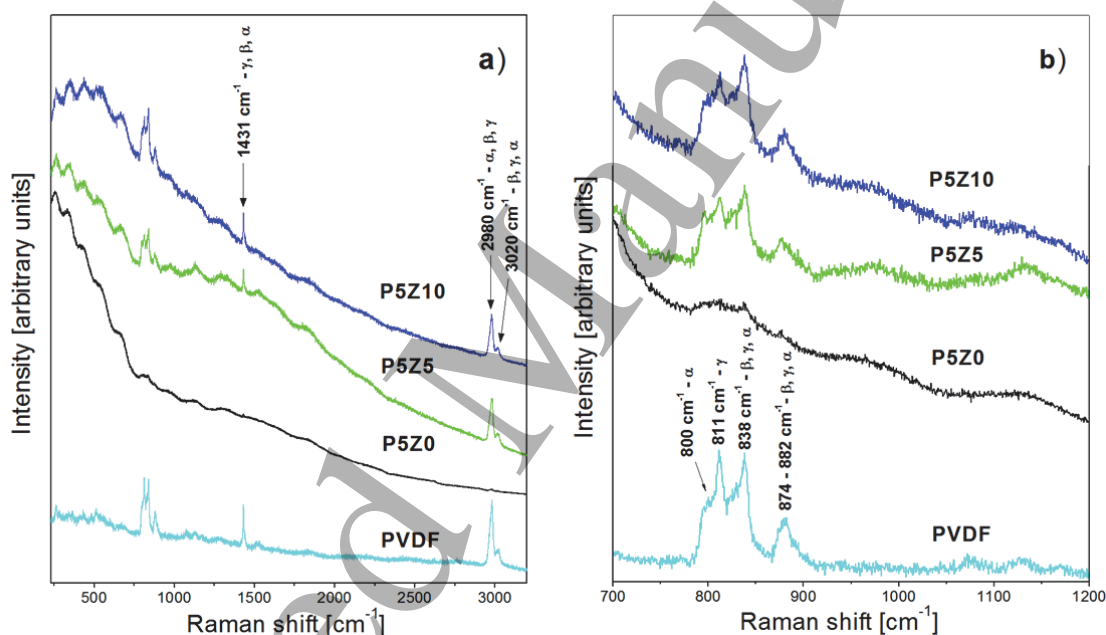

Figure 4. a) Raman spectra of PVDF and PVDF-ZnO composites with 5wt.% of the fillers mechanically activated for various activation times. b) The same spectra in the region from 700 to 1200 cm⁻¹.

Figure 4 shows Raman spectra of PVDF and the composites (with 5 wt.% of filler). The most pronounced changes in the Raman spectra were observed in the range from 750 - 900 cm⁻¹. In order to better illustrate these effects, the spectra are shown in the range from 700 – 1200 cm⁻¹ (Figure 4b). The analysis of the Raman spectrum of PVDF suggested that γ-phase is dominant: peak at ~ 811 cm⁻¹ is pronounced, which is typical of high content of γ-phase [42, 43]. Peaks at ~ 838 cm⁻¹, ~ (874 – 882) cm⁻¹ and ~ 1431 cm⁻¹ may originate from all three phases (α, β and γ), however, in the spectrum of the pure γ-phase, the line at ~ 1431 cm⁻¹ is very strong, unlike the corresponding lines in the spectra of α- and β-phase, suggesting that the main contribution to the line at ~ 1431 cm⁻¹ in our spectrum comes from γ-phase. The fact that one of the strongest lines in the Raman spectrum of the pure α-phase at ~ 800 cm⁻¹ is present only as a shoulder in our spectrum indicates that the peaks at ~ 838 cm⁻¹ and ~ 1431 cm⁻¹ should be assigned primarily to the β and γ phases [42-

45]. Furthermore, the peak at ~ 1431 cm^{-1} is more intensive than the broad peak at $\sim (874 - 882)$ cm^{-1} – in accordance with the assumption of the dominance of γ phase.

The analyses of the Raman spectra of the composites showed that non-activated ZnO filler reduces crystallinity of the polymer. The intensity of crystalline polymer lines generally decreases in P5Z0 sample and strong peaks at 1431 cm^{-1} and 2980 cm^{-1}, which represent the combination of all three crystalline phases, almost disappear (Figure 4). The decrease in intensity of the peaks at ~ 811 cm^{-1} (the γ phase) and ~ 838 cm^{-1} (primarily β and γ phase) is larger than that of the α peak at ~ 800 cm^{-1}, indicating a reduction in the contribution of γ and β phases. Raman spectra of the PVDF-ZnO composites with fillers activated for short times (5 and 10 min) show that mechanical activation results in significant changes in crystalline morphology of the PVDF matrix. The results suggest that the presence of activated ZnO particles induces a general rise in the intensity of crystalline polymer lines and an enhancement of β-phase crystallization in PVDF. In the spectra of P5Z5 and P5Z10 samples (Figure 4) the intensity of the line at ~ 811 cm^{-1} (the γ phase) decreases relative to the intensity of the peak at ~ 838 cm^{-1}. Having in mind that the strongest α line at 800 cm^{-1} is still relatively weak, the peak at ~ 838 cm^{-1} can be attributed primarily to the contribution of β and γ phases. Furthermore, taking into account that an increase in intensity of the peak at ~ 838 cm^{-1} occurs if the excess of β phase is present in the sample [43], the observed change in peak-height ratio of 811 cm^{-1} peak to 838 cm^{-1} peak is most likely due to enhanced formation of β crystals. This indicates that the particles mechanically activated for 5 and 10 min act as nucleation agents for β phase crystallization in PVDF.
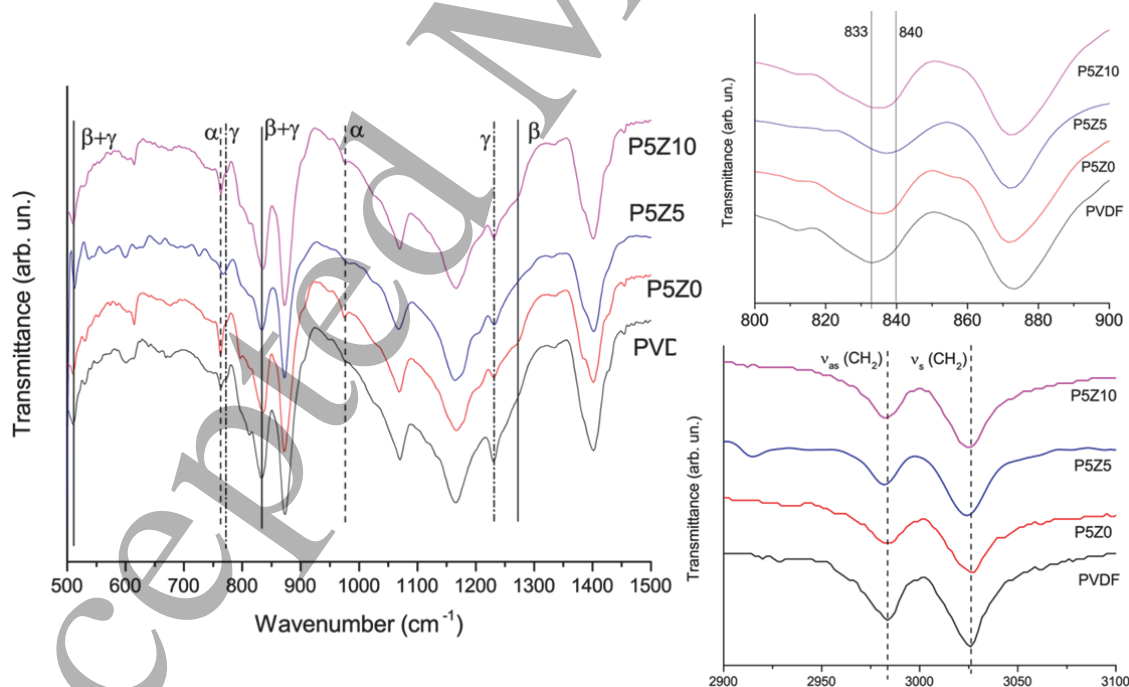

Figure 5. FTIR spectra of pure PVDF and samples with non-activated (P5Z0) and activated ZnO fillers (P5Z5 and P5Z10). Smaller sections show enhanced 800-900 cm^{-1} and 2900-3100 cm^{-1} regions.

Fourier-transform infrared (FTIR) spectra of pure PVDF and PVDF-ZnO composites show that the pure PVDF is synthesized as predominantly γ-phase with prominent peaks at 833 and 1234 cm^{-1} (Figure 5). Introduction of ZnO filler promotes crystallization of α- and β-phases, with reduction in content of γ-phase and overall reduction in crystallinity of the samples. The presence of α-phase is established from peaks at 766 and 976 cm^{-1}, while β-phase is identified using peaks at 840 and 1279 cm^{-1}. Enhancement of region from 800 to 900 cm^{-1} in Figure 5 shows that there is a shift in the position of maximum of the peak at 833 cm^{-1} towards 840 cm^{-1} in samples with ZnO fillers, suggesting formation of β-phase [44], which is supported by a shift in the position of CH_2 modes in this region towards lower energies, similar to what was observed in PVDF doped with gold nanoparticles [45]. Lower intensities of the peaks and lower shift of CH_2 modes suggests that the content of crystalline β-phase is most likely lower than α- and γ- phases, and overall FTIR spectrum suggests that both PVDF and PVDF-ZnO composite generally exhibit relatively poor crystallinity of the PVDF phase. However, FTIR indicates that the introduction of ZnO filler supresses the crystallization of γ-phase and promotes crystallization of α- and β-phases. The apparent differences between the Raman and FTIR results can be attributed to the fact that Raman spectroscopy only probed the surface of the PVDF/ZnO composite films, which is where the effects of strain on PVDF fibers is the most pronounced. This is also indicated by the fact that PVDF sample with non-activated filler exhibits extremely poor Raman spectrum, while its FTIR spectrum is not much different than that of other samples. This suggests that the distribution of phases in the PVDF/ZnO films would be inhomogeneous, with β-phase being more prevalent at the surface of the film, due to increased strain favoring its formation, with α-phase occurring mostly on the inside of the film.
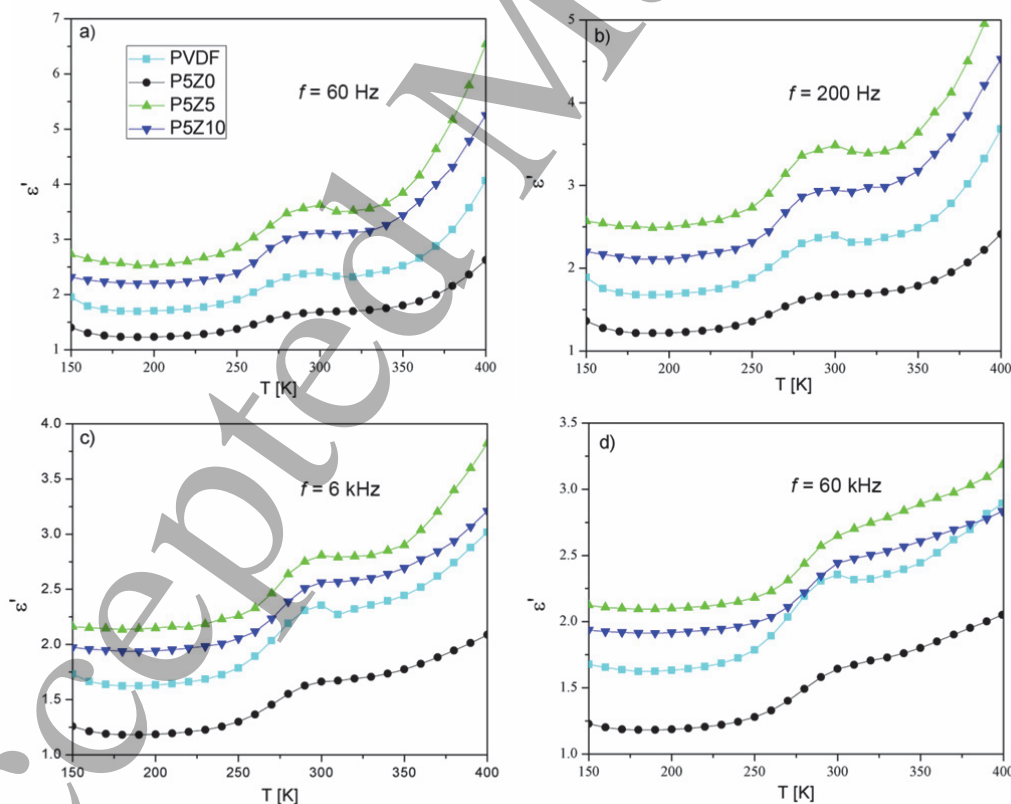

Figure 6. Dielectric permittivity (ε') *vs*. temperature curves for the pure PVDF and P5Z0, P5Z5, and P5Z10 composites measured at several frequencies: a) 60 Hz, b) 200 Hz, c) 6 kHz and d) 60 kHz

8

All four materials exhibit typical dielectric behaviour of PVDF e.g. at fixed frequency of the external field, the dielectric permittivity increases with increasing in temperature [46]. Also, the broad dielectric permittivity peak shifts to a higher temperature as the frequency increases, which is typical for a relaxation process in ferroelectrics [47]. On the other hand, the effects of the non-activated and activated ZnO particles on the dielectric permittivity of the polymer are different. The introduction of mechanically activated ZnO powders into the matrix leads to an increase in the dielectric permittivity of the polymer in the entire temperature range. In contrast, the composite with the commercial ZnO powder as a filler exhibits lower value of the dielectric permittivity than the pure PVDF (Fig. 6). This behaviour is a direct consequence of different crystallization behaviour of the PVDF matrix in the presence of these two type of fillers. Since inorganic content in the composites is the same (5 wt.%), an increase in dielectric permittivity can be related to a higher content of β-phase crystals in the composites with activated fillers (Fig. 4) [48, 49]. The fact that the dielectric permittivity of the composite with non-activated ZnO powder is lower than that of the pure PVDF suggests that the introduction of the particles with higher dielectric permittivity into PVDF matrix is not the sole condition for improvement of dielectric permittivity of the polymer. Rather, the dielectric properties will depend on the change in the PVDF matrix crystal polymorphism during the crystallization in the presence of the particles as well as on the strength of the interaction of the fillers and matrix chains. Finally, the results in Fig. 6 show that the composite with the ZnO filler mechanically activated for 5 min exhibits the highest dielectric permittivity, suggesting that this is the optimal activation time of the filler prior to mixing with the polymer matrix. It seems that prolonged mechanical activation has a detrimental effect on the surface activity of the particles, which results in their reduced activity as nucleating agents within the polymer matrix. Loss tangent curves that correspond to the dielectric permittivity (ε') curves in Fig.6 are shown in Fig. 7.

Table II. Values of dielectric permittivity and loss tagent for different frequencies at 300K and 400K.

| Sample 60Hz	T=300K dielectric permittivity	loss tangent	T=400K dielectric permittivity	loss tangent	α_c – onset (K)
PVDF	2.400	0.005	4.060	0.251	330
P5Z0	1.690	0.005	2.630	0.218	330
P5Z5	3.630	0.050	6.540	0.388	310
P5Z10	3.110	0.056	5.250	0.431	310
200Hz					
PVDF	2.395	0.058	3.681	0.179	330
P5Z0	1.682	0.005	2.412	0.151	330
P5Z5	3.486	0.060	5.318	0.270	320
P5Z10	2.944	0.070	4.527	0.303	320
6kHz					
PVDF	2.355	0.010	3.017	0.073	350
P5Z0	1.663	0.009	2.088	0.049	350
P5Z5	2.807	0.060	3.822	0.163	340
P5Z10	2.562	0.040	3.209	0.132	330
60kHz					
PVDF	2.355	0.043	3.017	0.037	360
P5Z0	1.643	0.039	2.051	0.025	360
P5Z5	2.647	0.054	3.184	0.120	350
P5Z10	2.443	0.048	2.835	0.083	350
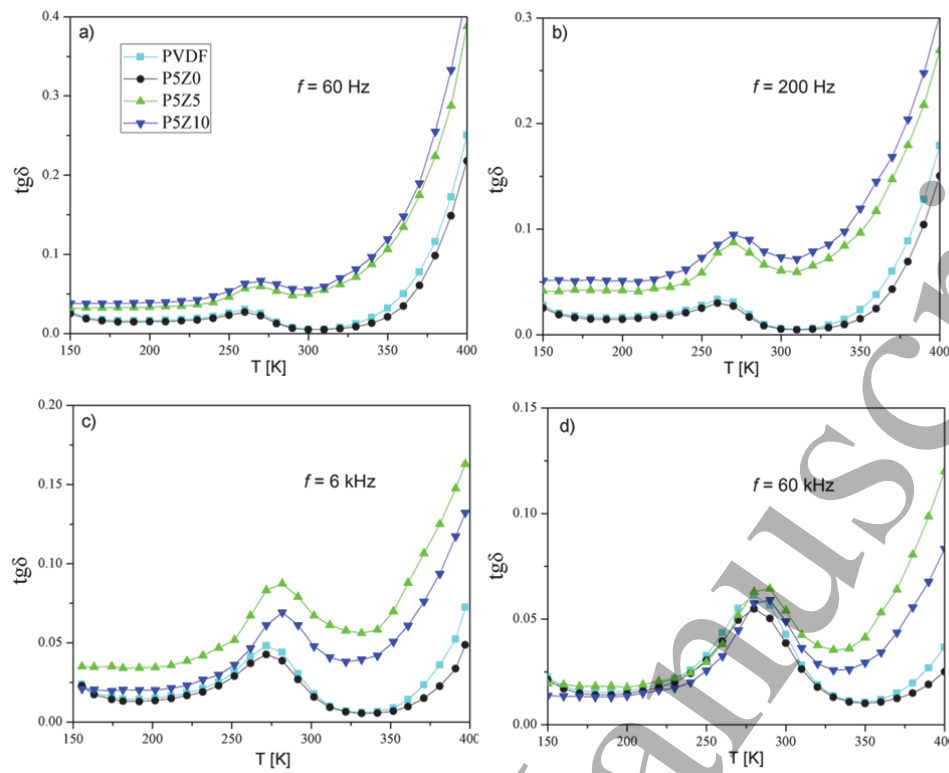
Figure 7. Loss tangent *vs.* temperature curves for the pure PVDF and P5Z0, P5Z5 and P5Z10 composites measured at several frequencies: a) 60 Hz, b) 200 Hz, c) 6 kHz and d) 60 kHz

All loss tangent curves show a typical low temperature relaxation observed at 200 K < T < 300 K [49], corresponding to glass transition processes of PVDF, involving crystalline and amorphous-crystalline regions. It is influenced by the composition and preparation of the composite [50]. The position of this relaxation peak shifts towards higher temperature (at fixed frequency of the external field) after introduction of mechanically activated particles. This indicates strong interaction of the activated particles and PVDF matrix chains, which reduces segmental mobility of PVDF chains and affects the cooperative motions in the polymer matrix, necessary for the glass transition to take place. Both dielectric permittivity and loss tangent curves exhibit a sharp increase at temperatures above 325 K, which is more pronounced at lower frequencies and in the composites with activated fillers (Figures 6 and 7). It most likely contains contributions from multiple processes, like electrode polarization processes [51] and α_c-transition [52]. Electrode polarization is a consequence of the accumulation of the charges at the surface of the electrode while under the force of the electric field. The electrode processes usually mask Maxwell–Wagner–Sillars (MWS) polarization processes, which are typical for heterogeneous systems and occur through polarizations at the interfaces of the constituents. The shift of the onset of the increase of dielectric permittivity to higher temperatures with increase in frequency is typical of α_c-transition [53, 54], which is indicated by the decrease in maximum value of dielectric loss at the end of the temperature interval at 400K with increase in frequency (Table II). In addition, the onset of α_c-transition appears to shift towards lower temperatures in samples containing mechanically activated fillers, compared to pure PVDF and the sample with non-activated filler. This indicates that the mechanical activation of the filler reduces the perfection of the lamellar PVDF crystals, making α_c-transition easier [55, 56], leading to lower crystallinity of PVDF in the samples containing activated fillers.
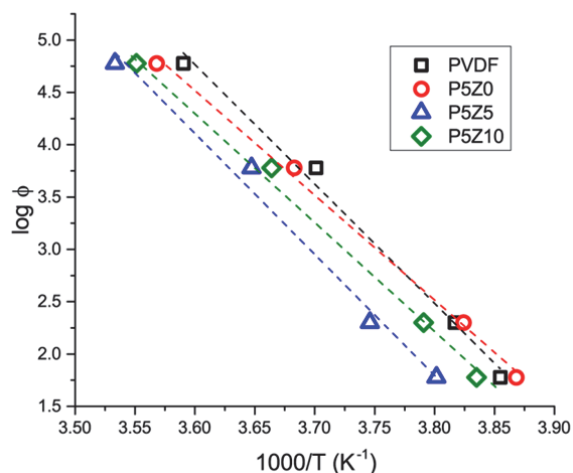
Figure 8. Arrhenius plots for the pure PVDF and P5Z0, P5Z5 and P5Z10 composites.

In order to determine whether strong particle-chain interaction was also reflected in the change in activation energy of this transition, the values of overall activation energy of the relaxation peak were calculated, since its position shifts to higher temperatures with increase in frequency, allowing the application of Arrhenius equation,

$$\phi = \phi_0 e^{-E_a/RT}, \tag{1}$$

where ϕ is the frequency used for measurement of dielectric permittivity, R is the universal gas constant, T is the position of the peak maximum and E_a is the overall average activation energy of the transition. According to Eq. 1, E_a is calculated from the slope of the plot $\log \phi = f(1/T)$. Fig. 8 shows the obtained Arrhenius plots for the pure PVDF and P5Z0, P5Z5 and P5Z10 composites. The activated energies (E_a) of the relaxation peak determined from the linear regression of the plots in Fig. 8 are presented in Table III. These suggest that the introduction of activated fillers in the PVDF matrix probably increases the value of the average activation energy, which would be consistent with the strong particle-chain interaction in these composites.

Table III. The overall average activation energy values of the low temperature relaxation processes, calculated from the linear regression of the plots in Fig. 8

Sample	E_a (kJ mol^{-1})
PVDF	206 ± 8
P5Z0	214 ± 8
P5Z5	223 ± 9
P5Z10	221 ± 9

Conclusions

Surface modification of ZnO nanoparticle fillers by means of mechanical activation has pronounced effect on the structural properties of the PVDF polymer matrix. TEM and SEM analyses showed that mechanical activation reduces particle size, and Raman and FTIR measurements showed that ZnO particles mechanically activated for short time (5 and 10 min) influence the crystallization of PVDF in different way than

11

non-activated ZnO particles. Non-activated ZnO filler decreases the crystallinity of the PVDF matrix and slightly increases the content of the α phase. On the other hand, PVDF-ZnO composites with 5 and 10 min activated fillers contain more β (ferroelectric) phase. These results, together with our previously published work [37, 38], show that mechanical activation of ceramic and semiconductor fillers prior to mixing with PVDF matrix can be used as general method for the fabrication of β-phase rich composite films. Dielectric spectroscopy measurements showed that the introduction of mechanically activated ZnO fillers resulted in an increase in dielectric permittivity, most likely due to an increase in β-phase content, while the introduction of non-activated ZnO powder resulted in a decrease in dielectric permittivity, likely due to the disruption of crystallization of PVDF matrix caused by the filler. The position of the broad relaxation peak in tan δ spectra of the composites with activated fillers shifted towards higher temperatures with respect to its position in the pure polymer. This suggests strong interaction of activated particles and polymer chains, due to a combination of increased surface area and increased concentration of surface defects in the activated fillers. This would be consistent with the obtained values of the activation energies of the relaxation peak via Arrhenius equation.

Acknowledgments

References

[1] D. A. Seiler, PVDF in the chemical process industry. In: Scheirs J, editor. Modern fluoropolymers, Wiley, Chichester, 1997. pp. 487–505.
[2] G. W Taylor, J. J. Gagnepain, T. R. Meeker, T. Nakamura, L. A. Shuvalov, Piezoelectricity, Gordon and Breach Science Publishers, New York, 1985.
[3] Q. Xunlin, J. Appl. Phys. 108 (2010), 011101
[4] Y. J. Park, Y. S. Kang, C. Park, Eur. 41 (2005), pp. 1002–1012
[5] A. J. Lovinger, Science 220 (1983), pp. 1115-1121.
[6] J. S. Humphrey, R. Amin-Sanayei, editors. Vinylidene fluoride polymers; Encyclopedia of Polymer Science and Technology, Wiley, New York (2002)
[7] T. Furukawa, Phase Transit. 18 (1989), pp. 143-211.
[8] K. Matsushige, K. Nagata, S. Imada, and T. Takemura, Polym. J. 21 (1980), pp. 1391-1397.
[9] G. T. Davis, J. E. McKinney, M. G. Broadhurst, and S. C. Roth, J. Appl. Phys. 49 (1978), pp. 4998-5002.
[10] K. Matsushige and T. Takemura, J. Polym. Sci., Polym. Phys. Ed. 16 (1978), pp. 921-934.
[11] C. Leonard, J. L. Halary, and L. Monnerie, Macromolecules 21 (1988), pp. 2988-2994.
[12] D. Shah, P. Maiti, E. Gunn, D. F. Schmidt, D. D. Jiang, C. A. Batt, and E. P. Giannelis, Adv. Mater. 16 (2004), pp. 1173-1177.
[13] S. Ramasundaram, S. Yoon, K. J. Kim, J. S. Lee, and C. Park, Macromol. Chem. Phys. 210 (2009), pp. 951-960.
[14] C. W. Tang, B. Li, L. Sun, B. Lively and W. H. Zhong, Eur. Polym. J. 48 (2012), pp. 1062-1072
[15] A. B. da Silva, J. Marini, G. Gelves, U. Sundararaj, R. Gregório Jr. and R. E. S. Bretas, Eur. Polym. J. 49 (2013), pp. 3318-3327
[16] K. Shehzad, A. Ul-Haq, S. Ahmad, M. Mumtaz, T. Hussain, A.Mujahid, A.T. Shah, M. Y. Choudhry, I. Khokhar, S. Ul-Hassan, F. Nawaz, F. ur Rahman,Y. Butt, M. Pervaiz, J Mater Sci 48 (2013) pp. 3737–3744
[17] A. Bahrami, Z. A. Talib, W. M. M. Yunus, K. Behzad, N. Soltani, Adv. Mat. Res. Vol. 364 (2012), pp 50-54
[18] L.L. Sun, B. Li, Z.G. Zhang, W.H. Zhong, Eur. Polym. J. 46 (2010), pp. 2112-2119
[19] S. Ducharme, ACS Nano. 3, (2009), pp. 2447-2450.

[20] P. Kim, S. C. Jones, P. J. Hotchkiss, J. N. Haddock, B. Kippelen, S. R. Marder, and J. W. Perry, Adv. Mater. 19 (2007), pp. 1001-1005.

[21] P. Kim, N. M. Doss, J. P. Tillotson, P. J. Hotchkiss, M.-J. Pan, S. R. Marder, J. Li, J. P. Calame, and J. W. Perry, ACS Nano 3 (2009), pp. 2581-2592.

[22] J. Li, J. Claude, L. E. Norena-Franco, S. I. Seok, and Q. Wang, Chem. Mater. 20 (2008), pp. 6304-6306.

[23] Ben-Hui Fan, Jun-Wei Zha, Dong-Rui Wang, Jun Zhao, Zhong-Feng Zhang, Zhi-Min Dang, Compos. Sci. Technol. 80 (2013), pp. 66–72

[24] Y. Niu, K. Yu, Y. Bai, H. Wang, IEEE Trans Ultrason Ferroelectr Freq Control, 62 (2015) pp. 108-115

[25] N. Kamezawa, D. Nagao, H. Ishii, M. Konno, Eur. Polym. J. 66 (2015), 528-532

[26] Z. L. Wang, J. Phys. Condens. Matt. 16, (2004), pp. R829-R858.

[27] L. Dong, Z. L. Cui and Z. K. Zhang, Nanostruct. Mater. 8 (1997), pp. 815–823.

[28] D. Ginley, C. Bright, MRS Bulletin, 25 (2000), pp. 15-18.

[29] K. Haraa, T. Horiguchib, T.Kinoshitab, K. Sayamaa, H. Sugiharaa, H. Arakawaa, Sol. Energ. Mat. Sol. C. 64 (2000), pp. 115–134.

[30] K. Keis, L. Vayssieres, S. Lindquist, A. Hagfeldt, Nanostruct. Mater. 12 (1999), pp. 487–490.

[31] I. M. Alibe, K. A. Matori, E. Saion, A. M. Ali, M. H. M. Zaid, The Influence of Calcination Temperature on Structural and Optical Properties of ZnO Nanoparticles via Simple Polymer Synthesis Route, Sci. Sinter. 49 (2017), 263-275

[32] A. P. Indolia, M. S. Gaur, J. Polym. Res. 20 (2013), p. 43.

[33] A. P. Indolia, M. S. Gaur, J. Therm. Anal. Calorim. 113 (2013), pp. 821–830.

[34] V. S. Nguyen, D. Rouxel, B. Vincent, L. Badie, F. D. Dos Santos, E. Lamouroux, Y. Fort, Appl. Surf. Sci. 279 (2013), pp. 204– 211

[35] J. S. Dodds, F. N. Meyers and K. J. Loh, Smart. Struct. Syst. 12 (2013), pp. 055-071

[36] Y. Lu, J. Claude, B. Neese, Q. Zhang, Q. Wang, J. Am. Chem. Soc. 128 (2006), pp. 8120-8121

[37] T. G. Mofokeng, A. S. Luyt, V. P. Pavlović, V. B. Pavlović, D. Dudić, B. Vlahović, V. Djoković, J. Appl. Phys.115 (2014), 084109

[38] V.P. Pavlović, V.B. Pavlović, B. Vlahović, D.K. Božanić, J.D. Pajović, R. Dojčilović, V. Djoković, Phys. Scripta. T157 (2013), 014006

[39] V. P. Pavlović, J. Krstić, M. J. Šćepanović, J. Dojčilović, D. M. Minić, J. Blanuša, S. Stevanović, V. Mitić and V. B. Pavlović, Ceram. Int. 37 (2011), pp. 2513-2518

[40] K. Vojisavljević, M. Šćepanović, T. Srećković, M. Grujić-Brojčin, Z. Branković and G. Branković, J. Phys.: Condens. Matter. 20 (2008), pp. 475202

[41] A. Peleš, V.P. Pavlović, S. Filipović, N. Obradović, L. Mančić, J. Krstić, M. Mitrić, B. Vlahović, G. Rašić, D. Kosanović, V.B. Pavlović, J. Alloy. Compd. 648 (2015), pp. 971-979

[42] S. Satapathy, Santosh Pawar, P. K. Gupta and K. B. R. Varma, Bull. Mater. Sci. 34 (2011), pp. 727–733.

[43] T. Boccaccio, A. Bottino, G. Capannelli, P. Piaggio, J. Membrane. Sci. 210 (2002), pp. 315–329.

[44] P. Nallasamy and S. Mohan, Indian J. Pure. Appl. Phy. 43 (2005), pp. 821-827

[45] M. Kobayashi, K. Tashiro, and H. Tadokoro, Macromolecules 8 (1975), pp. 158–171

[43] S. Liu, S. Xue, W. Zhang, J. Zhai, G. Chen, J. Mater. Chem. A, 2 (2014), pp. 18040-18046

[44] P. Martins, A. C. Lopes, S. Lanceros-Mendez, Progr. Polym. Sci. 39 (2014) pp. 683-706

[45] D. Mandal, K. Henkel, D. Schmeißer, Mat. Lett. 73 (2012) pp. 123-125

[46] J. Fu, Y. Hou, M. Zheng, Q. Wei, M. Zhu, H. Yan, ACS Appl. Mater. Interfaces, 7 (44) (2015), pp 24480–24491

[47] P. B. Ishai, M. S. Talary, A. Caduff, E. Levy, Y. Feldman, Meas. Sci. Technol. 24 (2013), 102001

[48] V. Sencadas, R. Barbosa, J. F. Mano, S. Lanceros-Méndez, Ferroelectrics 294 (2003), pp. 61-71.

[49] M. Grimau, E. Laredo, A. Bello, N. Suarez, J. Polym. Sci. Part B Polym. Phys., 35 (1997), pp. 2483–2493

[50] B. E. El Mohajir, N. Heymans, Polymer 24 (2001), pp. 5661-5667

[51] R. Gregorio Jr., E. M. Ueno, J. Mater. Sci. 34 (1999), pp. 4489–4500

[52] L. Yang, H. Ji, J. Qiu, K. Zhu, B. Shao, J. Intel. Mat. Syst. Str. 25 (2014), pp. 858–864

[53] K. Omote, H. Ohigashi, J. Appl. Phys. 81(6) (1997), 2760

[54] E. Ozkazanc, H. Y. Guney, T. Oskay, E. Tarcan, J. App. Polym. Sci., 109 (2008) pp. 3878–3886

[55] L. Yu, P. Cebe, J. Polym. Sci. B, 47 (2009) pp. 2520–2532

[56] J. Mijovic, J. W. Sy, T. K. Kwei, Macromolecules 30 (1997) pp. 3042–3050